Raman-Assisted Brillouin Distributed Temperature Sensor Over 100 km Featuring 2 m Resolution and 1.2 °C Uncertainty

Xabier Angulo-Vinuesa, Sonia Martin-Lopez, Javier Nuño, Pedro Corredera, Juan Diego Ania-Castañon, Luc Thévenaz, *Member, IEEE*, and Miguel González-Herráez

(Invited Paper)

***Abstract*—Raman assistance in distributed sensors based on Brillouin optical time-domain analysis can significantly extend the measurement distance. In this paper, we have developed a 2 m resolution long-range Brillouin distributed sensor that reaches 100 km using first-order Raman assistance. The estimated uncertainty in temperature discrimination is 1.2 °C, even for the position of worst contrast. The parameters used in the experiment are supported by a simple analytical model of the required values, considering the main limitations of the setup.**

***Index Terms*—Brillouin scattering, distributed optic fiber sensor, distributed Raman amplification, Raman scattering, temperature sensor.**

I. Introduction

DISTRIBUTED detection of temperature and strain along standard optical fibers is possible due to several techniques. Among them, Brillouin optical time-domain analysis (BOTDA) [1], [2] has evolved into a consolidated fiber sensing technology that is now widely used in different application domains (civil engineering, pipelines, fire detection, etc.).

The underlying physical phenomenon in this technology is a nonlinear optical effect called stimulated Brillouin scattering (SBS) [3]. This effect is an acousto-optic process that manifests as a narrowband amplification of a counterpropagating probe beam when an intense coherent pump light beam is introduced through one end of a single-mode fiber (SMF). To provide the distributed characteristic to the BOTDA, the pump wave is pulsed and the detected probe signal is analyzed as a function of the time of flight of the pump pulse in the fiber.

The measurement range and the spatial resolution are two of the most restrictive features of these systems, being generally limited to 20–30 km, with 1–2 m resolution [4]. On one hand, the measurement range is limited by the fiber attenuation, which causes an increase in the measurement uncertainty toward the end of the fiber. This is due to the fact that the attenuation reduces the gain experienced by the probe which leads to a smaller contrast and worse SNR. On the other hand, the resolution is set by the length of the pulses used to produce the distributed interaction. The use of short optical pulses increases the resolution, but at the same time the effective distance for amplification is reduced and the measurement uncertainty is increased due to the associated spectral broadening of the interaction. It is necessary then to find a proper balance between the resolution and the measurement range to comply with the required system specifications for each application.

Several studies have proven that the fiber losses can be successfully compensated using first or second-order distributed Raman amplification [5]–[7], leading to an enhancement of the measurement range without compromising the resolution. In [6], a measurement range of 75 km was demonstrated in a Raman-assisted BOTDA with a resolution of 2 m. In [7], the measurement distance was increased to 100 km with 2 m resolution, however using a more complicated second-order setup. In these works [6], [7], the relative intensity noise (RIN) of the Raman pumps and its transfer to the Brillouin signals was identified as the main issue to be solved in future improvements. In a recent work by Soto *et al.* [8], an increase of the range up to 120 km was demonstrated, keeping the resolution in 2 m with an estimated temperature uncertainty of 2.1 °C. The key improvement that allowed an enhanced performance in terms of sensing range was the low RIN of the Raman pumps copropagating with the probe. However, the sensing performance was demonstrated in the far end of the fiber, where the measurement contrast is not the minimum possible, and the demonstrated uncertainty remains high for some applications. In this paper, we present a first-order Raman-assisted BOTDA

Manuscript received June 30, 2011; revised September 08, 2011; accepted September 08, 2011. Date of publication September 22, 2011; date of current version March 02, 2012. This work was supported in part by the Spanish Ministry of Science and Innovation through Project TEC2009-14423-C02-01 and Project TEC2009-14423-C02-02, the Ministerio de Fomento through projects MIFFO (FOM-07/77) and IFZONE (FOM 39/08), and the Comunidad de Madrid through project FACTOTEM2. The work of X. Angulo-Vinuesa was supported by FACTOTEM2. The work of S. Martin-Lopez and J. Nuño was supported by the Spanish Ministry of Science and Innovation through a "Juan de la Cierva" Contract and an FPI Fellowship.

X. Angulo-Vinuesa, S. Martin-Lopez, J. Nuño, P. Corredera, and J. D. Ania-Castañon are with the Instituto de Óptica, Consejo Superior de Investigaciones Científicas, Madrid 28006, Spain (e-mail: xabier.angulo@io.cfmac.csic.es; soniaml@io.cfmac.csic.es; javier.nuno@io.cfmac.csic.es; pcorredera@io.cfmac.csic.es; juan.diego@io.cfmac.csic.es).

L. Thévenaz is with the Institute of Electrical Engineering, Ecole Polytechnique Fédérale de Laussane, Laussane CH-1015, Switzerland (e-mail: luc.thevenaz@epfl.ch).

M. Gonzalez-Herraez is with the Departamento de Electrónica, Universidad de Alcalá, Edificio Politécnico, Madrid 28871, Spain (e-mail: miguelg@depeca.uah.es).

Color versions of one or more of the figures in this paper are available online at http://ieeexplore.ieee.org.

Digital Object Identifier 10.1109/JLT.2011.2168807

sensor that features a 100 km range keeping the resolution in 2 m and achieving an estimated uncertainty of 1.2 °C (which is already adequate for pipeline monitoring). We explain some key improvements over the experimental setup reported in [6] that allow us to achieve this enhanced performance. We also provide a simple design methodology to analyze the requirements of this setup in terms of pump and probe powers, pump pulse extinction ratio, and Raman pump power. We show that this simple analysis gives a good approximation of the actual values needed for optimum performance.

II. Analysis of Requirements

In this section, we analyze some specific requirements to be taken into account when targeting long-range setups, in particular for ranges of 100 km and beyond. Through simple arguments, we derive the limit values that let us avoid extinction ratio, depletion, self-phase modulation (SPM), and RIN transfer issues in our setup. In what follows, the pump (P_B^+) is launched in the measured fiber at $z = 0$ and the probe (P_B^-) is launched in the fiber at $z = L$.

A. Extinction Ratio

In conventional BOTDA setups, the Brillouin pump pulse is obtained by external modulation of a master laser using an electro-optic modulator. In the "off" state, the modulator leaks a certain amount of pump power, characterized by the extinction ratio of the modulator. Even though this leakage is small, it may have a very significant impact on the measurement when targeting long ranges and high resolutions. Although the continuous wave (CW) power leaked by the modulator is orders of magnitude smaller than the pump pulse, its relative importance in the measurement comes from the fact that, the gain created by this CW background is distributed along the whole fiber length (100 km in this paper) while the amplification created by the pump pulse remains limited to the resolution of the measurement (2 m in this paper).

For small gains, one can treat this nonideality as a superposition of the ideal case (short pulse with infinite extinction ratio) with a CW background generated by the continuous amplification of the probe by the CW background of the pump. Using the analysis performed in [6] for the Raman-assisted configuration we can only quantify the signal to background ratio numerically. However, we can easily understand the requirements in terms of extinction ratio by comparing a conventional setup and a perfectly transparent Raman-assisted configuration (with effectively zero loss, similar to the configurations reported in [7]).

For a conventional setup, the worst case of signal to background ratio is obtained in the far end of the fiber (where the pump is more attenuated), and is given by

$$\frac{\Delta P_B^-\big|_{\text{pulse}}}{\Delta P_B^-\big|_{\text{leak}}} = \frac{\Delta z \exp(-\alpha L)}{\kappa L_{\text{eff}}} \tag{1}$$

where ΔP_B^- is the detected change in probe wave power, α is the fiber attenuation, κ is the extinction ratio of the modulator, Δz is the pump pulse length, L is the fiber length, and L_{eff} is the effective length, as conventionally defined. In the aforementioned expression, we have assumed that the change on the Brillouin probe is small in all cases and that the fiber is perfectly homogeneous.

For the best results, this contrast should be made as high as possible. We can nevertheless obtain a good tradeoff by setting this ratio to ≥ 1. For a conventional 20 km setup with 2 m resolution and $\alpha = 0.2$ dB/km, the aforementioned expression implies extinction ratios already in the order of 40 dB. These are still attainable with conventional electro-optic modulators.

As mentioned before, we cannot find analytically this ratio in a Raman-assisted configuration. However, for comparison, we can find a similar expression for a perfectly transparent fiber (this regime is very similar to the second-order configuration demonstrated in [7])

$$\frac{\Delta P_B^-\big|_{\text{pulse}}}{\Delta P_B^-\big|_{\text{leak}}} = \frac{\Delta z}{\kappa L}. \tag{2}$$

An analysis of this expression shows that Raman assistance is less stringent in terms of extinction ratio requirements. For comparison, with the same criterion as previously, a 100 km setup with 2 m resolution requires extinction ratios of 47 dB in the case of perfect Raman assistance (complete transparency) and 60 dB in the conventional nonassisted case. These values are anyway not conventional in electro-optic modulators (although possibly attainable in acousto-optic modulators). The improvement in this issue in the case of Raman assistance comes from the fact that the contrast is kept constant along the fiber, while it diminishes toward the fiber end in conventional setups.

In the setup employed in this paper, we significantly enhance the signal to background ratio. This is done by introducing an additional device after the modulator (a nonlinear optical loop mirror, NOLM [9]) to enhance the extinction ratio of the pulses. This device works as a saturable absorber: the transmission grows with the power. In the working range, the output of this device scales with the cube of the input power [9], leading in theory to a tripling of the extinction ratio in decibel. In practice, however, the extinction ratio achieved is limited (by Rayleigh scattering and other nonidealities) to approximately 60 dB. For comparison, the results in [6] over 75 km with 2 m resolution were obtained with an electro-optic modulator featuring 43 dB extinction ratio.

B. Depletion

In [6], it was recognized that depletion issues were the main source of nonideality in the Raman-assisted case. Until recently, an analytical model of depletion in BOTDA sensors was not available. In the last months, Foaleng-Mafang *et al.* [10] developed a simple analytical model of pump depletion in conventional BOTDA. Although the model developed in [10] is not adapted to the Raman-assisted case, we can again have an idea of the required parameters in our system by comparing the two cases treated in the previous section: the conventional case and the case of perfect transparency.

According to [10], the fraction of power lost by the pump through depletion can be directly calculated from the theoretical Brillouin loss induced by the probe; hence

$$d = \frac{P_{Bo}^+ - P_B^+}{P_{Bo}^+} = 1 - \exp\left(-\frac{g_B}{A_{\text{eff}}} P_B^-(L) L_{\text{eff}}\right) \tag{3}$$

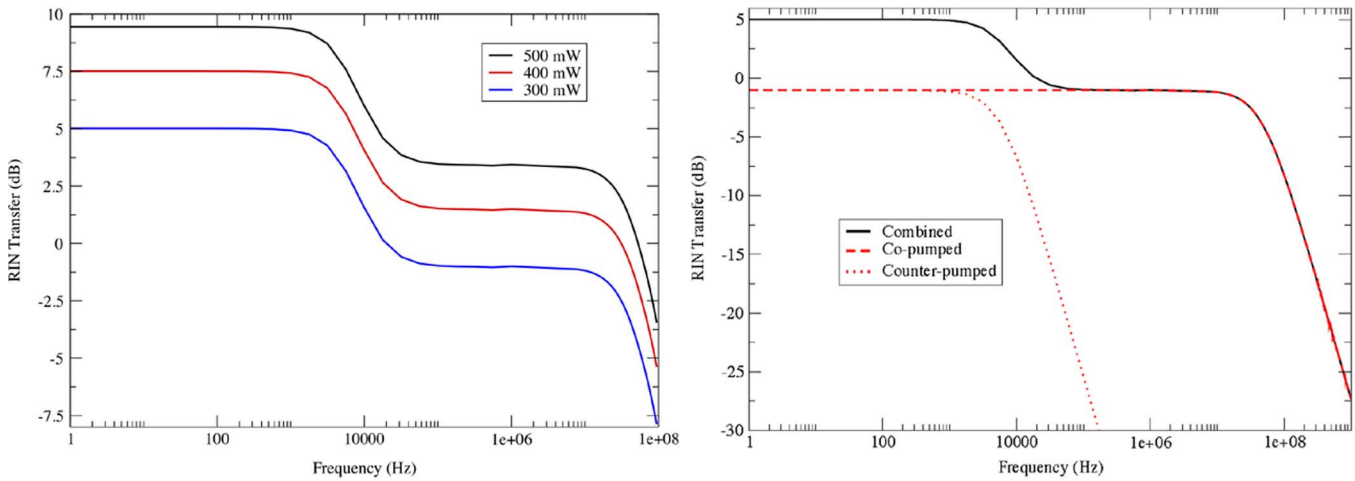

Fig. 1. (a) RIN transfer as a function of the Raman pump power for a 100 km fiber span for several pump powers. (b) Detail of the RIN transfer as a function of frequency estimated for the copropagating and counterpropagating configurations in relation with the bidirectional case (all the fiber parameters are the same as those used in [6]).

where P_{Bo}^{+} is the pump power in absence of Brillouin interaction, g_B is the Brillouin gain coefficient, and A_{eff} is the effective area of the fiber. This expression comes from the fact that the gain on the probe can be considered negligible in all cases. For a perfectly transparent setup (similar to [7]), we can obtain a similar expression by simply replacing L_{eff} by L. We can now set the acceptable depletion to values below 10%. It has been shown that this gives acceptable frequency errors below 1 MHz [10]. For the typical fiber characteristics ($g_B = 5 \cdot 10^{-11}$ m/W, $A_{\text{eff}} = 70\ \mu\text{m}^2$) and $L = 100$ km, we can infer that one has to work at power levels in the order of 1 μW or below in the Raman-assisted configuration (in conditions of perfect transparency), while one can reach up to 7 μW in the conventional nonassisted one.

C. SPM

SPM has been shown to play a nonnegligible detrimental role in BOTDA sensors, particularly in long-range and high-resolution setups. SPM leads to small phase chirps during intensity transitions in the pump pulse (leading and trailing edges) that eventually become important in long fibers. The frequency broadening associated with this phase modulation leads to a reduced peak gain and uncertainties in the determination of the Brillouin shift, but leaves the temporal intensity distribution of the pump pulse unchanged, hence the spatial resolution is preserved. As shown in [11], for a Gaussian pulse with a $1/e$ width τ, the peak excursion of the instantaneous frequency is given by $\Delta\omega_{\max} = 2\gamma P z_{\text{eff}}/\sqrt{e}\tau = 1.43\,\gamma P z_{\text{eff}}/T$, where T is the full-width at half-maximum of the pulse. For a perfectly transparent setup, the effective length in the previous expression should be replaced by the physical length of the fiber. We can preserve a good contrast along the fiber by bounding the maximum broadening to 10 MHz. In the perfectly transparent case, this limits the pump power to approximately 1.4 mW. In a nonassisted configuration, the power limit to avoid significant spectral broadening in the pump could remain at approximately 6 mW.

D. RIN Transfer

In previous works on Raman-assisted BOTDA [12]–[14], RIN transfer was identified as a major limitation in the performance. Here, we analyze more deeply the effect of RIN transfer on the performance of BOTDA, in particular with regards to the pump power and pumping scheme. From this analysis we will derive a maximum Raman pump power in our setup beyond which the Raman assistance ceases to be effective in improving the signal quality.

RIN transfer in the BOTDA setup is analyzed by employing the model developed in [12]. In our case, this model is used to quantify RIN transfer as a function of the pump power in a bidirectionally pumped scheme as a function of signal frequency (within the detection bandwidth, roughly 100 MHz), total pump power (from both ends), and pumping scheme. The results for a standard single-mode optical fiber are shown in Fig. 1. The BOTDA signals (pump and probe) are spectrally located at 1554 nm and the Raman pumps at 1455 nm. All the fiber parameters are the same as those used in [6]. More specifically, Fig. 1(a) shows the evolution of RIN transfer as a function of the Raman pump power for a 100 km fiber span and Fig. 1(b) is a comparison of the 300 mW case with the cases of copropagating and counterpropagating pumping with 150 mW.

As expected, the logarithmic RIN transfer increases very rapidly with power. In the bidirectional configuration, the RIN transfer curve shows a low-pass shape with two characteristic cutoff frequencies, one in the kilohertz range and the other in the tens of megahertz range. As shown in Fig. 1(b), the shape of the RIN transfer curve can be seen as the vector sum of the copropagating and counterpropagating cases, the counterpropagating one (with respect to the probe) showing a much lower cutoff frequency. This agrees well with the intuitive picture of copropagating amplification, in which the pump and the signal travel with similar group velocities, favoring RIN transfer over a wider frequency range. The main limitation in terms of noise in this configuration is thus imposed by the pump power copropagating with the probe.

Considering a typical RIN value of Raman lasers of -110 dBc/Hz, the expected RMS noise in this case is expected

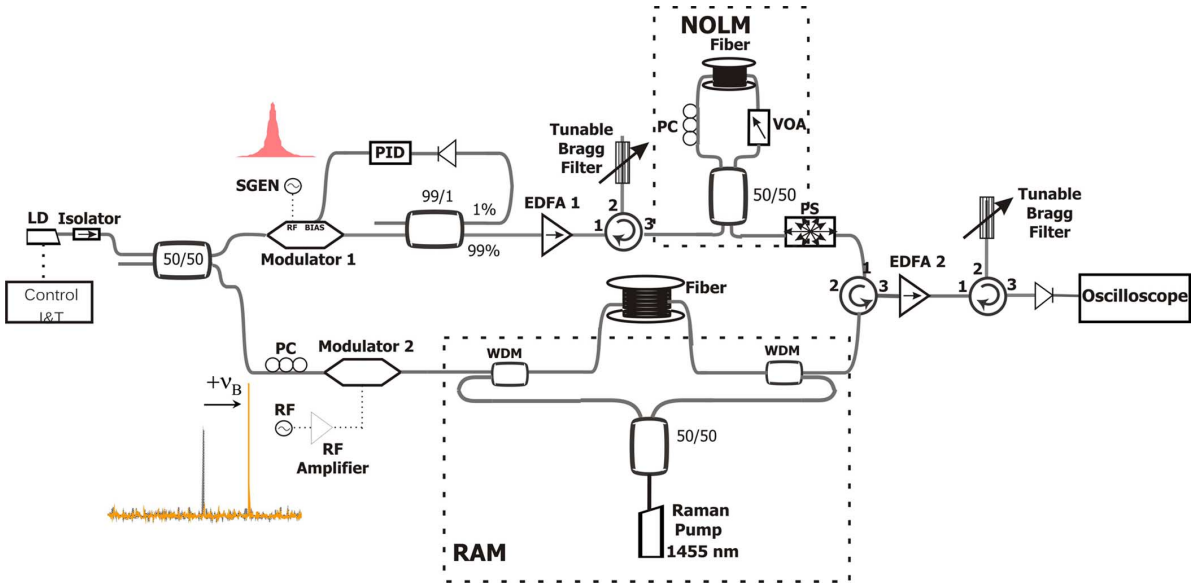

Fig. 2. Experimental setup of the Raman-assisted distributed Brillouin sensor. LD: laser diode; PC: polarization controller; SGEN: pulse generator; PI: proportional-integral electronic circuit; EDFA: erbium-doped fiber amplifier; RF: radio-frequency generator; NOLM: nonlinear optical loop mirror; PS: polarization scrambler; WDM: wavelength division multiplexer.

to be in the order of 10^{-3}, which is in the same order as the gain to be measured. As one increases the Raman pump power, the overall RIN doubles at approximately 420 mW and triples at powers slightly below 500 mW. The growth of RIN transfer is thus faster than the achieved gain. Hence, one should only use Raman amplification up to the point of overcoming the detection issues. To avoid RIN issues one should therefore employ low-RIN pumps like the setup described in [8] or pump just up to the point of making the signal visible within the range of the detection setup. This is actually the approach used in this paper.

III. Experimental Setup

The setup employed for this work is depicted in Fig. 2, and is similar to the one reported by some of the authors of this paper in [6]; however, this one has a couple of key improvements in the pulse generation setup and the Raman pump tuning. Pump and probe signals are generated with a controlled frequency difference from a unique source that is split and modulated [15]. This scheme avoids that any frequency disturbance on the master source affects the frequency difference between the pump and probe signals. The master source of our BOTDA (see Fig. 2) is a 4 mW laser diode (LD) ($\sim$ 1 MHz linewidth), which emits at 1553.59 nm. The pump is pulsed with 30 ns pulses, which are amplified by an erbium-doped fiber amplifier (EDFA). Since the measurement distance is 100 km, the repetition rate of the pulses has to be lower than 1 ms, which means that a very low duty cycle is used (in the order of 10^{-5}). It is necessary then to achieve extinction ratios in the order of 10^5 to be able to measure properly the variations on the probe wave. Two systems are used to ensure this extinction ratio in the pump. First, an electronic proportional-integrator (PI) circuit is employed in the modulator to set the working point. The PI sets the working point of the modulator to minimum transmission, which allows 25–30 dB of extinction. Since this is not good enough considering the figures given in Section II, an NOLM [9] is employed after the pulse shaping and the amplification. The NOLM provides the necessary extinction to achieve >50 dB of extinction in the pump pulse. The NOLM also produces a small compression of the pulses obtaining a pedestal-free narrow pulse [9], [16], which alters the original 30 ns width to approximately 20 ns. Thus, 20 ns pump pulses with a repetition rate of 700 Hz are supplied to the fiber.

The probe signal is obtained from the lower frequency sideband of the amplitude-modulated master source. The modulation frequency is scanned around the Brillouin shift of the fiber under test ($\sim$ 10.68 GHz). The carrier frequency is suppressed by properly setting the dc bias of the modulator, and the higher frequency sideband is filtered before detection. Both sidebands propagate in the fiber under test, which compensates the depletion of the pump signal by the detected probe (lower sideband), thus making the system very robust to depletion-induced errors [10].

In order to achieve SBS, both pump and probe signals are introduced in the sensing fiber in opposite directions together with the Raman pumps through suitable wavelength division multiplexers (WDMs). The Raman pumps are obtained by splitting the output of a Raman fiber laser (RFL). Thus, a bidirectional configuration is used for the Raman amplification process [13], [14]. The RFL emits at 1455 nm, which induces Raman amplification in the region of 1550 nm. The maximum power of the RFL can reach 2.4 W, although we only used 480 mW (240 mW through each side). This Raman pump power is below the value needed for a perfect end-to-end compensation of the losses (so generally lower than the pump levels used in [6]); however, it guarantees the best tradeoff between amplification and RIN transfer for our RFL in this fiber segment, as shown in the previous section. To mitigate the polarization sensitivity of the interaction, a polarization scrambler (PS) is employed, and before detection the probe signal is amplified by another EDFA.

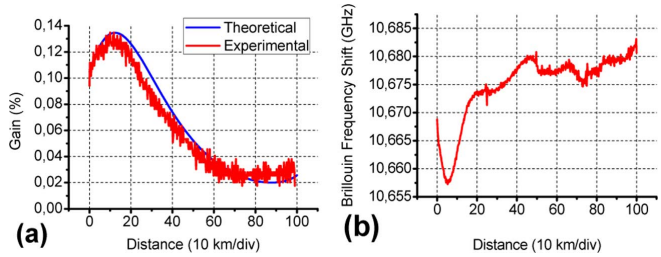

Fig. 3. (a) Comparison between the obtained maximum gain trace at each position (red line) and the calculated results using the analytical model of the bidirectional Raman-assisted configuration [6]. (b) Evolution of the Brillouin frequency shift along the 100 km of optical fiber.

IV. Results

In this section, we illustrate the results obtained with the Raman-assisted BOTDA configuration described previously, as well as calculated results obtained with an analytical model developed previously [6]. The 100 km fiber is composed by four SMF spools of 25 km with an effective area of 70 μm^2 and a similar Brillouin frequency shift located at approximately 10.67 GHz for the pump wavelength ($\sim$ 1554 nm). The peak power of pump and probe were 2.133 mW and 0.17 μW, respectively, with 480 mW of Raman pump. This is comparable (or even lower) than the values used in [6] for the bidirectional configuration over 75 km. Fig. 3(a) shows a comparison between the measured and calculated gain (with the model developed in [6]) at each point of the fiber. We can observe the good agreement between both traces, which verifies the proper operation of the system. As mentioned, the pump power used is slightly below the value necessary for a good compensation of the losses. However, this ensures a good behavior of the setup in terms of RIN. As can be seen, the power levels used are in good agreement with the simple derivations provided in the previous section, hence providing a first-hand analytical idea of the values to be used for optimum performance.

In Fig. 3(b), the evolution of the retrieved Brillouin frequency shift all along the sensing distance is depicted. The evolution of the frequency shift is comprised between 10.6725 and 10.6825 GHz. The variation of ν_B along the first kilometers is most probably due to some longitudinal variation in the construction parameters of the fiber (probably the GeO_2 doping). The difference in the retrieved Brillouin shift along the fiber in consecutive measurements is smaller than 1.5 MHz, which means a temperature uncertainty below 1.2 °C.

Fig. 4 shows a representation of the full frequency sweep obtained for this fiber. It is noticeable that the gain as a function of the frequency fits the expected Gaussian/Lorentzian profile [3], and no depletion is visible. The maximum gain contrast is achieved at approximately 15 km of the fiber input while the minimum gain contrast is obtained around 80 km. From here onward, the gain contrast keeps increasing until the end of the fiber.

To demonstrate that our BOTDA is accurate even in the worst conditions, we decided to locate a hot spot in between the last two fiber spools, where the gain contrast is minimal. 2.5 m of fiber were introduced in a water bath at 55 °C ($\pm$5 °C), with a room temperature of 21 °C. Fig. 5 shows the frequency sweep performed around the hot-spot location. We can clearly see the hot-spot location at the expected position (roughly 74.83 km).

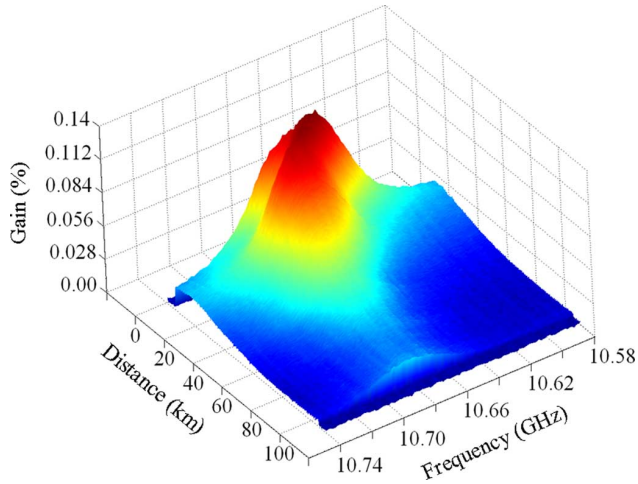

Fig. 4. Full gain sweep showing the measurement over the complete measuring distance, 100 km.

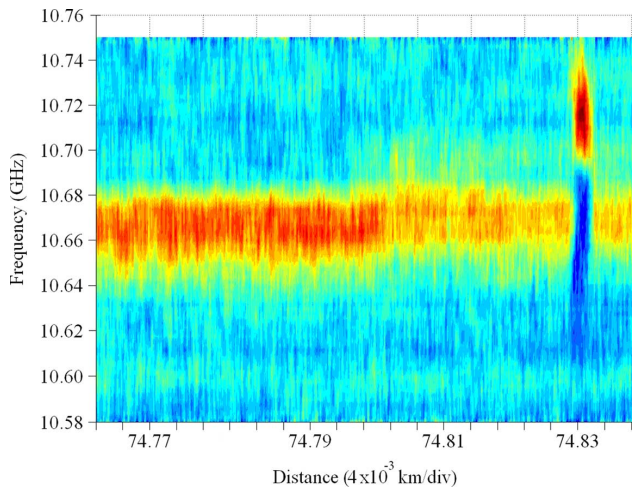

Fig. 5. Brillouin gain sweep around the hot spot (located close to 75 km). Frequency is swept between 10.58 and 10.75 GHz.

We can also observe the transition between the third and fourth fiber spool at approximately 74.80 km. The frequency difference between the hot spot and the rest of the fiber sections is approximately 45 MHz. Considering the sensitivity of 1.3 MHz/°C in the Brillouin shift, this gives us a temperature variation of 35 °C, which is in good agreement with the expected temperature difference.

V. Conclusion

We have presented a distributed optical fiber sensor with 2 m resolution and 100 km range. We have shown that the system performs correctly as a temperature sensor by demonstrating accurate determination of the temperature in a hot spot even in the position with minimal gain contrast. In comparison with our previous configuration, we have achieved a range extension of 25 km keeping the same resolution. This was achieved using lower pump, probe, and Raman power levels compared to [6], which led to a significantly reduced RIN transfer from the Raman pump to the Brillouin probe. Additionally, a much better extinction ratio in the pump pulse was achieved by using an NOLM. The quality of the results makes us believe that it

could be possible to achieve longer measuring distances by applying higher power levels with more precise settings and lower RIN pumps. Additionally, we have shown a simple method to analyze the requirements of a long-range Brillouin setup for a correct operation, in particular to avoid extinction ratio, SPM, depletion, and RIN transfer issues. The optimum values found experimentally agree well with the expectations of this simple model, allowing a first-hand evaluation of the values to be used.

REFERENCES

[1] T. Horiguchi and M. Tateda, "Optical-fiber-attenuation investigation using stimulated Brillouin scattering between a pulse and a continuous wave," *Opt. Lett.*, vol. 14, no. 8, pp. 408–410, 1989.

[2] T. Horiguchi and M. Tateda, "BOTDA—Nondestructive measurement of single-mode optical fiber attenuation characteristics using Brillouin interaction: Theory," *J. Lightw. Technol.*, vol. 7, no. 8, pp. 1170–1176, Aug. 1989.

[3] G. P. Agrawal, *Nonlinear Fiber Optics*, 4th ed. San Diego, CA: Academic, 2007, ch. 9.

[4] M. Niklés, "Fibre optic distributed scattering sensing system: Perspectives and challenges for high performance applications," presented at the presented at the Third Eur. Workshop Opt. Fiber Sens., Napoli, Italy, 2007.

[5] M. N. Alahbadi, Y. T. Cho, and T. P. Newson, "150-km-range distributed temperature sensor based on coherent detection of spontaneous Brillouin backscatter and in-line Raman amplification," *J. Opt. Soc. Amer. B*, vol. 22, no. 6, pp. 1321–1324, 2005.

[6] F. Rodríguez-Barrios, S. Martín-López, A. Carrasco-Sanz, P. Corredera, J. D. Ania-Castañón, L. Thévenaz, and M. González-Herráez, "Distributed Brillouin fiber sensor assisted by first-order Raman amplification," *J. Lightw. Technol.*, vol. 28, no. 15, pp. 2162–2172, Aug. 2010.

[7] S. Martín-López, M. Alcón-Camas, F. Rodríguez, P. Corredera, J. D. Ania-Castañón, L. Thévenaz, and M. González-Herráez, "Brillouin optical time-domain analysis assisted by second-order Raman amplification," *Opt. Exp.*, vol. 18, no. 18, pp. 18769–18778, 2010.

[8] M. A. Soto, G. Bolognini, and F. Di Pasquale, "Optimization of long-range BOTDA sensors with high resolution using first-order bi-directional Raman amplification," *Opt. Exp.*, vol. 19, pp. 4444–4457, 2011.

[9] N. J. Doran and D. Wood, "Nonlinear-optical loop mirror," *Opt. Lett.*, vol. 13, no. 1, pp. 56–58, 1988.

[10] L. Thevenaz, S. F. Mafang, and J. Lin, "Impact of pump depletion on the determination of the Brillouin gain frequency in distributed fiber sensors," presented at the presented at the 21st Int. Conf. Opt. Fiber Sensors, Ottawa, Canada, 2011.

[11] S. M. Foaleng-Mafang, F. Rodriguez-Barrios, S. Martin-Lopez, M. Gonzalez-Herraez, and L. Thévenaz, "Detrimental effect of self-phase modulation on the performance of Brillouin distributed fiber sensors," *Opt. Lett.*, vol. 36, pp. 97–99, 2011.

[12] C. R. S. Fludger, V. Handerek, and R. J. Mears, "Pump to signal RIN transfer in Raman fiber amplifiers," *J. Lightw. Technol.*, vol. 19, no. 8, pp. 1140–1148, Aug. 2001.

[13] R. H. Stolen and E. P. Ippen, "Raman gain in glass optical waveguides," *Appl. Phys. Lett.*, vol. 22, pp. 276–278, 1972.

[14] J. Bromage, "Raman amplification for fiber communications systems," *J. Lightw. Technol.*, vol. 22, no. 1, pp. 79–93, Jan. 2004.

[15] M. Niklés, L. Thévenaz, and P. A. Robert, "Brillouin gain spectrum characterization in single-mode optical fibers," *J. Lightw. Technol.*, vol. 15, no. 10, pp. 1842–1851, Oct. 1997.

[16] J. Wu, Y. Li, C. Lou, and Y. Gao, "Optimization of pulse compression with an unbalanced nonlinear optic mirror," *Opt. Commun.*, vol. 18, pp. 43–47, 2000.

Xabier Angulo-Vinuesa was born in Bilbao, Spain, in 1982. He received the Electronics Engineer Degree from the University of the Basque Country, Bilbao, in September 2009. He is currently working toward the Ph.D. degree at the Optics Institute, Spanish Council for Research, Madrid, Spain.

During 2008–2009, he had a stay in the Interdisciplinary Nanoscience Centre, Aarhus University, Denmark, where he was involved in photonic crystal waveguides. His research interests include nonlinear fiber optics and fiber optic sensors.

Sonia Martin-Lopez received the Ph.D. degree from the Universidad Complutense de Madrid, Madrid, Spain, in May 2006, with focus on experimental and theoretical understanding of continuous-wave pumped supercontinuum generation in optical fibers.

She had a long stay in the Nanophotonics and Metrology Laboratory, Ecole Polytechnique Federale de Lausanne, Switzerland. She is currently a Postdoctoral Researcher in the Applied Physics Institute, Spanish Council for Research, Madrid. She is the author or coauthor of 70 papers in international refereed journals and conference contribution. Her research interest includes nonlinear fiber optics.

Javier Nuño was born in Aranda de Duero, Spain, in 1983. He received the telecommunications degree from Universidad de Valladolid, Valladolid, Spain, and the Master degree in laser technology from Universidad Politécnica de Madrid, Madrid, Spain, in 2007 and 2009, respectively. He is currently working toward the Ph.D. degree in the Instituto de óptica, Spanish Council for Research, Madrid, Spain.

In 2007, he had a long stay in the Photonics Research Group, Aston University, U.K. His research interests include the exploitation of nonlinear effects in optical systems.

Pedro Corredera received the B.Sc. and Ph.D. degrees in physics from the University of Salamanca, Salamanca, Spain, in 1985 and 1989, respectively.

In 1996, he joined the Institute of Applied Physics, CSIC, Madrid, Spain, where he is currently a Research Manager of the Fibre Optics Laboratory. His research interests include fiber-optic measurements, optical fiber sensors, nonlinear fiber optics, and IR radiometry and detection.

Juan Diego Ania-Castañón was born in Oviedo, Spain, in 1973. He received the M.Sc. degree in physics from Universidad Complutense de Madrid, Madrid, Spain, in 1996, and the Ph.D. degree in theoretical physics from Universidad de Oviedo and Instituto de Estructura de la Materia, Consejo Superior de Investigaciones Científicas (CSIC), Madrid, Spain, in 2000.

In 2001, he joined the Photonics Research Group, Aston University, Birmingham, U.K., first as a Contract Research Fellow and then as an Engineering and Physical Sciences Research Council Advanced Research Fellow from 2004. In 2007, he joined as a Tenured Scientist at the Instituto de Óptica, CSIC. His main research interests include the study of nonlinear dynamics in optical systems and the exploitation of nonlinear effects in optical fiber.

Luc Thévenaz (M'02) received the M.Sc. degree in astrophysics from the Observatory of Geneva, Geneva, Switzerland, in 1982, and the Ph.D. degree in physics from the University of Geneva, Geneva, in 1988 (with expertise in fiber optics).

In 1988, he joined the Swiss Federal Institute of Technology of Lausanne (EPFL), Switzerland. In 1991, he visited the PUC University, Rio de Janeiro, Brazil, and Stanford University, Stanford, CA, where he was involved in the development of a Brillouin laser gyroscope. In 1998 and 1999, he stayed at the Korea Advanced Institute of Science and Technology, Daejeon, Korea, where he was involved in fiber laser current sensors. He leads currently a Research Group at the EPFL that is involved in photonics, in particular, fiber optics and optical sensing. His research interests include electrical current fiber sensors, Brillouin scattering fiber sensors, fiber nonlinearities measurement techniques, and laser-diode spectroscopy of gases.

Miguel González-Herráez received the M.Eng. and D.Eng. degrees from the Polytechnic University of Madrid, Madrid, Spain, in 2000 and 2004, respectively.

He joined as a Research Assistant and then became a Postdoctoral Fellow in the Applied Physics Institute, Spanish Council for Research, Madrid, Spain, and had several long stays in the Nanophotonics and Metrology Laboratory, Ecole Polytechnique Federale de Lausanne, Switzerland. In October 2004, he joined as an Assistant Professor in the Department of Electronics, University of Alcalá, Madrid, Spain, where he became an Associate Professor in June 2006. He is the author or coauthor of more than 100 papers in international refereed journals and conference contributions and has given several invited talks at international conferences. His research interests include the wide field of nonlinear interactions in optical fibers.